Seventh International Conference on CFD in the Minerals and Process Industries
CSIRO, Melbourne, Australia
9-11 December 2009

2-D NEWTONIAN FLOW PAST ELLIPSOIDAL PARTICLES AT MODERATE REYNOLDS NUMBERS

N. N. KUMAR and N. KISHORE*

Department of Chemical Engineering, National Institute of Technology Warangal – 506004, INDIA
*Corresponding Author: Email: mail2nkishore@gmail.com, Tel.: +91-870-2462626

ABSTRACT

The flow of steady, isothermal and incompressible viscous fluids past different shaped solid particles has been a subject of interest due to their many applications in chemical and metallurgical industries. This work presents numerical results on the flow of Newtonian fluids past spheroidal particles over the following range of parameters; Reynolds number, Re, $1 \leq Re \leq 500$ and aspect ratio, e, $0.5 \leq e \leq 2.5$. The present results obtained by using Fluent 6.0. The accuracy of the present results is ascertained by comparing the present drag values with the literature values. It has been observed that the streamlines and vorticity contours; the surface pressure coefficients and vorticity magnitudes are also seen to be strongly dependent on Reynolds number and aspect ratio. Regardless of the value of the aspect ratio, the individual and total drag coefficients decrease with increasing values of Reynolds numbers. The effect of the shape of particles on individual and total drag coefficients is small at low Reynolds numbers but as increasing the Reynolds number the effect magnifies. As the Reynolds number increases, the pressure to friction drag ratio increases; however, the effect of aspect ratio is more significant for $e > 1$ rather than for $e \leq 1$.

NOMENCLATURE

a Particle diameter in the flow direction (m)
b Particle diameter in the direction normal to flow (m)
C_d Total drag coefficient (-)
C_{df} Friction drag coefficient (-)
C_{dp} Pressure drag coefficient (-)
e Aspect ratio factor (-)
P Pressure (N/m^2)
Re Reynolds number (-)
R_∞ Outer domain radius (m)
U_o Free settling velocity (m/s)
V_x x-component of velocity (m/s)
V_y y-component of velocity (m/s)
V_z z-component of velocity (m/s)

Greek symbols

μ Viscosity of fluid ($Pa\ s$)
ρ Density of fluid (kg/m^3)

INTRODUCTION

The phenomena of flow separation, wakes formation and drag behaviour in flow past various types of bluff bodies has acquired great interest amongst many researchers because of their fundamental significance in understanding the flow physics and their practical importance in hydrodynamic applications. In general, engineering applications often involve flows over simple and complex bluff bodies like spheres, cylinders, triangles; cubes, diamonds, ellipsoidal particles and other arbitrarily shaped solid particles. In such flows, parameters such as angle-of-attack can greatly influence the nature of separation and the wake structure. Therefore, a fundamental study of flow over complex shapes of ellipsoidal particles would significantly augment the current understanding of the physics of the flow and drag behaviour of flow past bluff bodies.

In recent years considerable effort has been directed at investigating the flow and drag behavior of various shapes of solid particles (spheres, cylinders, squares, etc.) settling in Newtonian liquids (Clift et al., 1978; Michaelides, 2006) and to some extent in non-Newtonian fluids (Chhabra, 2006). An inspection of the recent reviews of the pertinent literature shows that the sedimentation behavior of solid spheres, circular and square cylinders in Newtonian and followed by those in purely viscous fluids (mostly power-law) has been studied most thoroughly, at least, in the moderate range of pertinent parameters (Tonini and Lemcoff, 1981; Hu and Joseph, 1990; Phan-Thien and Dou, 1999; Mangadoddy, et al., 2004; Nakamura and Igarashi, 2004; Chhabra, 2006; Dhiman et al., 2006; Dhole et al., 2006). Based on a combination of the numerical and experimental studies, reliable results are now available on drag coefficient—Reynolds number behavior; flow separation and wake formation behaviour for spheres, circular cylinders and square cylinders falling in unconfined fluids up to about Reynolds number of 1000. On the other hand, ellipsoidal particles, which are more general geometrical configurations than the spherical or cylindrical particles and provide a richer flow behavior characteristic of typical engineering flow configurations. For these shapes, changes in aspect ratio ranging from $0.5 \leq e \leq 2.5$ allow for different shapes from disk-like ($e < 1$) to cylinder-like ($e > 1$) and includes spheres for which $e = 1$. But there is lack of systematic study pertaining to the flow and drag phenomenon of ellipsoidal particles in Newtonian liquids.

PREVIOUS WORK

There have been few studies available on flow of Newtonian liquids past ellipsoidal or spheroidal particles in limiting conditions. Analytical expressions for the drag force acting on prolates and oblates are available in creeping flow regime (Clift et al. 1978). Militzer et al. (1989) proposed a correlation for drag spheroidal particles in Newtonian media on the basis of the available experimental data. The steady and laminar flow past spheroids have been numerically studied by Masliyah and Epstein (1970) and Comer and Kleinstreuer (1995). Their results show that the surface pressure variations and drag coefficients are a strong function of the aspect ratio. Brenner (1996) presented a review on the settling of a

non-spherical particle in an infinite Newtonian fluid under creeping flow conditions. Blaser (2002) used the results obtained by Brenner (1996) to evaluate the hydrodynamic forces acting on an ellipsoidal particle immersed in various flow fields, like, constant, simple shear, two-dimensional straining and axisymmetric straining flow in the creeping flow region. Wen and Jog (2005) numerically studied the steady and varying thermo-physical property, continuum, and laminar thermal plasma flow over spheroidal particles. They observed that the effects of flow Reynolds number, particle shape, surface and far field temperatures and variable properties are greatly affect the flow and temperature fields around the particles. They reported drag values of spheroidal particles as function of particle surface temperature and free stream temperatures. However, drag results are not presented for the case of isothermal spheroidal particles. Tripathi et al. (1994) and Tripathi and Chhabra (1995) calculated the drag force on a spheroid moving in a power-law liquid in the convective flow regime. Broday et al. (1998) theoretically studied the motion of non-neutrally buoyant prolate spheroidal particles in vertical shear flows to calculate the hydrodynamic forces and moments acting on such inertial and inertialess particles and their trajectories. Hsu et al. (2005) have analytically studied the boundary effect on the drag force acting on a rigid non-spherical particle settling in a Carreau fluid in the low to moderate range of Reynolds numbers. Rajitha et al. (2006) experimentally obtained the free settling velocity of cylinders and disks falling in quiescent Newtonian and power-law liquids and proposed modification to the existing drag expression for spherical particles falling in Newtonian and power-law fluids by introducing a sphericity factor. There have also been studies on the evaluation of hydrodynamic force on the floc consisting either spherical particles (Hsu and Hseih, 2002) or spheroidal particles (Wu and Lee, 2001; Hsu and Hseih, 2003) for either of the cases of homogenous and non-homogenous porous flocs. However, there is no systematic study reported on the flow and drag phenomena of single ellipsoidal particles flowing in a quiescent Newtonian liquids in the moderate range of Reynolds numbers. Thus this work is aimed to fill this gap and provide an independent correlation to calculate the drag coefficient acting on ellipsoidal particle in a Newtonian liquid in the range of parameters $0.5 \le e \le 2.5$ and $1 \le Re \le 200$.

PROBLEM DESCRIPTION

Consider the steady, incompressible and two dimensional axisymmetric Newtonian flow past ellipsoidal particles. The problem has been schematically shown in Figure 1, wherein, ellipsodial particles of eccentric factor, $e = b/a$; ($e < 1$ and $e > 1$) are remained stationary in an unbounded Newtonian fluid flowing with a free stream velocity, U_o. Here the 'a' is the diameter of the particle in the direction of flow, whereas, the 'b' is the diameter of the particle in the direction normal to the flow as shown in Figure 1. Since the range of Reynolds number is 1-200, under which the flow remains axisymmetric, the computations have been carried out in the half domain only.

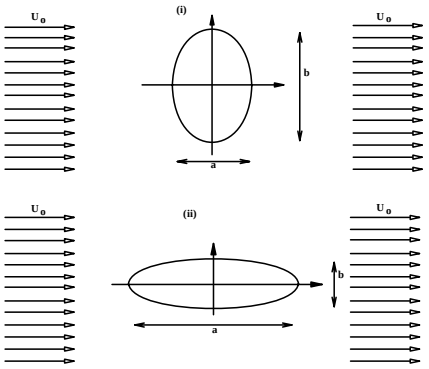

Figure 1. Schematic representation of the flow geometry.

Consider Cartesian coordinate system with the axis 'x' being directed along the flow direction and axis 'y' is in the direction normal to the flow. Due to the symmetry, $V_z = 0$ and no flow variable depends upon the z-coordinate. The flow characteristics in this problem are governed by the equations of conservation of mass and momentum. These governing equations in Cartesian coordinates in their dimensional form for an incompressible fluid can be written as follows:

- Equation of continuity:

$$\frac{\partial V_x}{\partial x} + \frac{\partial V_y}{\partial y} = 0 \qquad (1)$$

- x-component of momentum equation:

$$\rho\left(V_x \frac{\partial V_x}{\partial x} + V_y \frac{\partial V_x}{\partial y}\right) = -\frac{\partial p}{\partial x} + \mu\left(\frac{\partial^2 V_x}{\partial x^2} + \frac{\partial^2 V_x}{\partial y^2}\right) \qquad (2)$$

- y-component of momentum equation:

$$\rho\left(V_x \frac{\partial V_y}{\partial x} + V_y \frac{\partial V_y}{\partial y}\right) = -\frac{\partial p}{\partial y} + \mu\left(\frac{\partial^2 V_y}{\partial x^2} + \frac{\partial^2 V_y}{\partial y^2}\right) \qquad (3)$$

Equations (1) - (3) can be solved numerically using no-slip boundary condition on the surface of the particle, inlet velocity and outlet pressure boundary conditions along with the symmetry boundary condition in the flow direction along the symmetry line. All these ellipsoidal particles of different aspect ratio factor are subjected to a buoyancy force. While flowing, Skin friction (or viscous drag) and form drag (due to pressure distribution) are occurred due to relative velocity between the fluid and the solid object. Therefore, these governing equations along with the specified boundary conditions have solved using a finite volume method based computational fluid dynamics algorithm in order to obtain the steady velocity and pressure fields in the entire computational flow domain. These steady velocity and pressure fields can now be used for the post-processing such as to calculate the drag coefficients, streamlines and vorticity contours and to extract surface pressure distribution and surface vorticity magnitude distribution.

NUMERICAL DETAILS

Due to the complicated nature of the flow, theoretical analysis are typically limited to either flow at very low or very large Reynolds number. Experimental techniques have become very sophisticated in recent years; however, numerical simulations provide a promising approach to analyze such complex flow problems. However, there remain a number of issues that need to be addressed, namely intelligent grid generation, efficient solution of the

governing equations, etc. The accuracy of the numerical results is also contingent upon a prudent choice of the size of the outer domain and of an optimal grid which are strong function of Reynolds number. Here in this study, the Reynolds number, is defined based on the diameter of the particle in the direction normal to the flow, i.e., on the basis of 'b'.

$$\mathrm{Re} = \frac{(2b)U_o\rho}{\mu} \quad (4)$$

In order to obtain the steady state numerical velocity and pressure fields in the entire computational domain, Eqs. (1) - (3) have been solved using finite volume method based commercial CFD software Fluent 6.0. A mesh has been generated (for the flow geometry as shown in Figure 1) using Gambit and it has been called in Fluent 6.0. The convective terms of the momentum equation have been descritized using QUICK scheme and the temporal and viscous terms have been descritized using a central differencing scheme. The inlet velocity and outlet pressure boundary conditions are used at inlet and outlet boundaries. Thus obtained steady state velocity and pressure fields can now be used for the post-processing such as to calculate the drag coefficients, streamlines and vorticity contours and to extract surface pressure distribution and surface vorticity magnitude distribution.

Domain independence

The size of the domain is more critical at low values of the Reynolds numbers due to stronger viscous forces compared to convective forces. Table 1 summarizes the findings of the domain independence study for two extreme values of aspect ratio, i.e., e = 0.5 at Re = 1 and e = 2.5 at Re = 2.5 using three values of the domain sizes, R_∞ = 50, 150, 250. From this table, it is clear that almost all domain sizes produce results within < 1% for both extreme values of aspect ratio. Therefore, a domain of size R_∞ = 150 has been considered as an optimum domain.

Domain (R_∞)	C_{dp}	C_{df}	C_d
e = 0.5 at Re = 0.5			
50	5.2214	23.7870	29.0084
150	5.1232	23.7080	28.8312
250	5.3428	24.4783	29.8211
e = 2.5 at Re = 2.5			
50	17.7291	9.1377	26.8668
150	17.6809	9.1156	26.7965
250	17.6419	9.1001	26.7420

Table 1. Domain independence study for particles of e = 0.5 and e = 2.5.

Grid independence

Grid	C_{dp}	C_{df}	C_d
e = 0.5 at Re = 100			
90 × 400	0.1586	0.3962	0.5548
120 × 400	0.1586	0.3960	0.5546
120 × 300	0.1589	0.3960	0.5549
e = 2.5 at Re = 500			
90 × 400	1.0556	0.1258	1.1814
120 × 400	1.0554	0.1250	1.1804
120 × 300	1.0631	0.1257	1.1888

Table 2. Grid independence study for the optimum domain R_∞ = 150.

Having fixed an optimum domain, it is also necessary to choose an optimal grid size which represents a trade-off between the accuracy of the results and the computational requirements. Grid can be a sensitive factor for large Reynolds number flows due to increasing contribution of convection terms than the viscous terms, thus, grid independence study is to be carried out for large value of Reynolds number. Table 2 shown a summary of the grid independence study for two extreme values of aspect ratio, i.e., e = 0.5 at Re = 100 and e = 2.5 at Re = 500. Here too, any combination of any two grids produces results within < 1%, however, for the safer side a finer grid of size 120 × 400 has been chosen as the optimum grid for this flow study. Thus, now it is safe to say that the present results are free from numerical artifacts such as grid and domain independence.

RESULTS AND DISCUSSION

Before presenting the new results it is desirable to ascertain the accuracy and reliability of the present results by comparing them with the literature values. Table 3 shows a summary of comparison of the present values of drag coefficients of solid spheres (e = 1) in Newtonian liquid at Re = 1, 20, 200 with those of LeClair et al. (1970), Graham and Jones (1994), Saboni et al. (2004) and Dhole et al. (2006). It is clear from this table that the present results are seen to be within ± 2-3% of the literature values. Furthermore, differences of this magnitude are not at all uncommon in such numerical studies due to the differences stemming from grid errors, solution procedure, etc. (Roache, 1994). In view of these factors and based on our comparisons, the present results are believed to be reliable and accurate to within ± 2-4%.

Re	LeClair et al. (1970)	Graham and Jones (1994)	Saboni et al. (2004)	Dhole et al. (2006)	Present
1	27.37	27.767	27.55	26.13	27.056
20	2.736	2.663	2.768	2.692	2.7253
200	0.772	-	0.776	0.744	0.7708

Table 3. Comparison of the present values of the total drag coefficient (C_d) of a sphere.

Flow phenomena

Figure 2 shows the effect of Reynolds number on the streamline and iso-vorticity contours of ellipsoidal particles of aspect ratio, e = 2.5. The upper half of ellipse shows the streamlines while the lower half shows the iso-vorticity contours. At Re = 2.5, the streamlines in the front-half and rear-half are almost symmetric representing no separation zone. As the Reynolds number increases to Re = 125, due to the increased contribution of convection, there is a flow separation, the size of which further increases as the Reynolds number increases up to Re = 500. The iso-vorticity also being transferred along the flow direction as the Reynolds number increased due to the convection domination. Figures 3 and 4 shows the effect of the Reynolds number on the streamlines and iso-vorticity contours for spheroidal particles of aspect ratio, e = 1.5 and e = 0.5, respectively. Here too similar observations as in the case of e = 2.5.

Thus, in summary, for a fixed value of the Reynolds number, the size of recirculation increases with the

increase of aspect ratio. The ratio between the recirculation zones of spheroidal particles and a sphere is less than unity for $e < 1$ (disk like) and it is greater than unity for $e > 1$ (cylinder like).

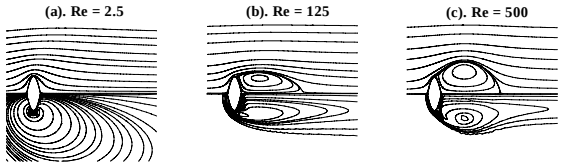

Figure 2. Effect of Reynolds number on streamlines and vorticity contours of ellipsoidal particle of aspect ratio, e = 2.5.

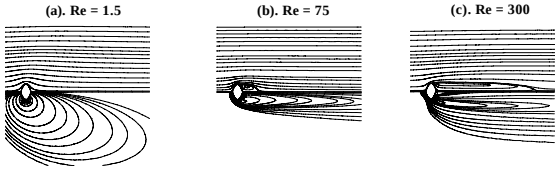

Figure 3. Effect of Reynolds number on streamlines and vorticity contours of ellipsoidal particle of aspect ratio, e = 1.5.

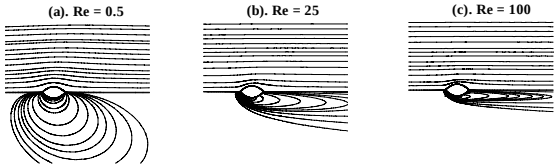

Figure 4. Effect of Reynolds number on streamlines and vorticity contours of ellipsoidal particle of aspect ratio, e = 0.5.

Distribution of pressure coefficient and vorticity magnitude

Figure 5 shows effects of the Reynolds number and aspect ratio on the dimensional pressure coefficient distribution on the surface of particles. For all values of the aspect ratio, the pressure coefficient is identical both in the front half of the particle as well as in the rear half due to negligible effect of the convection forces. This symmetry is strong for $e < 1$ and gradually some sort of asymmetry caused as the value increases to $e > 1$. However, for all values of the aspect ratio, as the Reynolds number increases, the pressure in the rear half gradually becomes much lesser compared to that in the front half of the particle due to the formation of recirculation zone. This difference is more in the case of particles with $e > 1$ rather than in particles with $e < 1$ as the flow separation is poor for particles of $e < 1$. On the other hand, at $Re \geq 10$, the effect of the Reynolds number is more predominant for particles of $e \geq 1$.

Figure 6 shows effects of the Reynolds number and aspect ratio on the dimensional vorticity magnitude distribution on the surface of particles. For all values of Reynolds numbers, similar trends were observed for particles with $e \geq 1$. These observations are consistent with those of spheres and cylinders. On the other hand, for particles with $e < 1$ (disk like), for all values of Reynolds numbers, at the front stagnation point some finite value observed which gradually falls to a minimum value close to zero as there is no separation.

In the case of $e = 1$ (spheres), for all values of Reynolds number, the trends are consistent with the literature trends (LeClair et al., 1970; Saboni et al., 2004; Feng and Michaelides, 2001). For $e = 1.5$, the trends are more or less similar to those of spheres for all values of Reynolds numbers. However, for $e = 2.5$, the vorticity magnitude in recirculation zone is much greater than in the front half of the particles especially for $Re = 250$ and $Re = 500$. This is due to the larger size of the recirculation zone than the size of the particle itself as witnessed in Figure 2 at these values of the Reynolds numbers.

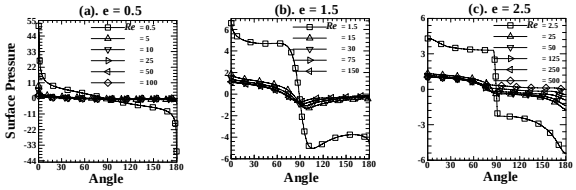

Figure 5. Effect of Re and e on the dimensional surface pressure coefficient.

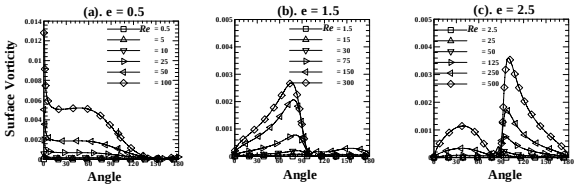

Figure 6. Effect of Re and e on the dimensional surface vorticity magnitude.

Drag phenomena

Figure 7 shows the effect of aspect ratio on the individual and total drag coefficients and on the pressure to friction drag ratio. Regardless of the value of aspect ratio, both individual and total drag coefficients decreases as the value of Reynolds number increases. However, effect of aspect ratio is more significant on pressure (form) drag coefficient rather on viscous and total drag coefficients. The effect of aspect ratio is negligible for $Re < 10$. For all values of Reynolds number, as the value of aspect ratio increases, the form drag coefficient increases, whereas, reverse trend observed in viscous drag coefficient. Furthermore, for all values of aspect ratio, the ratio between form drag and viscous drag increases as the value of the Reynolds number increases, but the effect is small for $e \leq 1$. For $e > 1$ (cylinder like), as the value of the Reynolds number increases, this ratio drastically increases. Thus, for any value of Reynolds number, the value of C_{dp}/C_{df} is small for $e < 1$ (disk like) and large $e > 1$ (cylinder like) compared to the case of $e = 1$ (sphere).

CONCLUSIONS

In this work, flow and drag phenomena of spheroidal particles have been investigated. It has been seen that regardless of the value of aspect ratio, the individual and total drag coefficients decrease with increasing values of Reynolds numbers. Further, it is seen that the effect of the shape of the particles on individual and total drag coefficients is small at low Reynolds numbers but as increasing the Reynolds number the effect magnifies. The effect of aspect ratio is more significant on pressure (form) drag coefficient rather on viscous and total drag coefficients. As the Reynolds number increases, the pressure to friction drag ratio increases; however, the effect of aspect ratio is more significant for $e > 1$ (cylinder like) rather than for $e < 1$ (disk like). Furthermore, the

streamlines and vorticity contours; the surface pressure coefficients and vorticity magnitudes are also seen to be strongly dependent on Reynolds number and aspect ratio. For fixed Reynolds number the size of recirculation increases with the increase of aspect ratio. The ratio between the recirculation zones of spheroidal particles and a sphere is less than unity for $e < 1$ (disk like) and it is greater than unity for $e > 1$ (cylinder like).

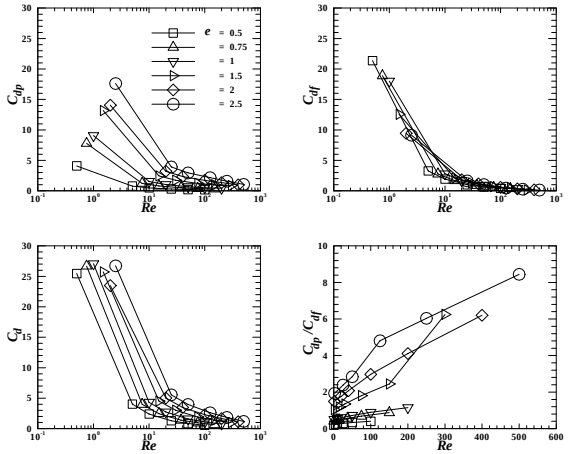

Figure 7. Effect of *Re* and *e* on the individual and total drag coefficients and on the ratio of pressure to friction drag coefficients.

REFERENCES

BIRD, R.B., STEWART, W.E. AND LIGHTFOOT, E.N., "Transport Phenomena", 2nd Edition, John Wiley, New York, (2002).

BLASER, S., Forces on the surface of small ellipsoidal particles immersed in a linear flow field, Chem. Eng. Sci., **57**, 515-526 (2002).

BRENNER, H., The Stokes hydrodynamic resistance of non-spherical particles, Chem. Eng. Commun., **148**, 487-562 (1996).

BRODAY, D., FICHMAN, M., SHAPIRO, M. AND GUTFINGER, C., Motion of spheroidal particles in vertical shear flows, Phys. Fluids, **10**, 86-100 (1998).

CHHABRA, R.P., "Bubbles, Drops, and Particles in Non-Newtonian Fluids", 2nd Edition CRC press, Boca Raton, FL, USA (2006).

CHHABRA, R.P., TIU, C. AND UHLHERR, P.H.T., A Study of wall effects on the motion of a sphere in viscoelastic fluids, Can. J. Chem. Eng., **59**, 771-775 (1981).

CLIFT, R., GRACE, J.R. AND WEBER, M.E., "Bubbles, Drops and Particles", Academic Press (1978).

COMER, J.K. AND KLEINSTREUER, C., A numerical investigation of laminar flow past nonspherical solids and droplets, J. Fluids Eng., **117**, 170-175 (1995).

DHIMAN, A.K., CHHABRA, R.P. AND ESWARAN, V., Steady flow of power-law fluids across a square cylinder, Chem. Eng. Res. Des., **84**, 300-310 (2006).

DHOLE, S.D., CHHABRA, R.P. AND ESWARAN, V., Flow of power-law fluids past a sphere at intermediate Reynolds numbers, Indus. Eng. Chem. Res., **45**, 4773-4781 (2006).

FENG, Z.G. AND MICHAELIDES, E.E., Heat and mass transfer coefficients of viscous spheres, Int. J. Heat Mass Transfr., **44**, 4445-4454 (2001).

GRAHAM, D.I. AND JONES, T.E.R., Settling and transport of spherical particles in power-law liquids at finite Reynolds number, J. Non-Newt. Fluid Mech., **54**, 465-488 (1994).

HAPPEL, J. AND BRENNER, H., "Low Reynolds Nuber Hydrodynamics", Academic Press, New York (1983).

HU, H.H. AND JOSEPH, D.D., Numerical simulation of viscoelastic flow past a cylinder, J. Non-Newt. Fluid Mech., **37**, 347-377 (1990).

HSU, J.P. AND HSIEH, Y.H., Drag force on a floc in a flow field: two layer model, Chem. Eng. Sci., **57**, 2627-2633 (2002).

HSU, J.P. AND HSIEH, Y.H., Drag force on a porous non-homogeneous spheroidal floc in a uniform flow field, J. Colloid and Interface Sci., **259**, 301-308 (2003).

HSU, J.P., HSIEH, Y.H. AND TSENG, S., Drag force on a rigid spheroidal particle in a cylinder filled with Carreau fluid, J. Colloid and Interface Sci., **284**, 729-741 (2005).

LECLAIR, B.P., HAMIELEC, A.E. AND PRUPPACHER, H.R., A numerical study of the drag on a sphere at intermediate Reynolds numbers, J. Atm. Sci., 27, 308-315 (1970).

MANGADODDY, N., PRAKASH, R., CHHABRA, R.P. AND ESWARAN, V., Forced convection in cross flow of power-law fluids over a tube bank, Chem. Eng. Sci., **59**, 2213-2222 (2004).

MASLIYAH, J.H. AND EPSTEIN, N., Numerical study of steady flow past spheroids, J. Fluid Mech., **44**, 513-528 (1970).

MICHAELIDES, E.E., "Particles, Bubbles and Drops: Their Motion, Heat and Mass Transfer", World Scientific, Singapore (2006).

MILITZER, J., KAN, J.M., HAMDULLAHPUR, F., AMYOTTE, P.R. AND AL TAWEEL, A.M., Drag coefficient for axisymmetric flow around individual spheroidal particles, Powder Technol., **57**, 193-195 (1989).

NAKAMURA, H. AND IGARASHI, T., Variation of Nusselt number with flow regimes behind a circular cylinder for Reynolds numbers from 70 to 30000, Int. J. Heat Mass Transfr., **47**, 5169-5173 (2004).

PHAN-THIEN, N. AND DOU, H.S., Viscoelastic flow past a circular cylinder: drag coefficient, Computer Methods in Appl. Mech. Engg., **180**, 243-266 (1999).

RAJITHA, P., CHHABRA, R.P., SABIRI, N.E. AND COMITI, J., Drag on non-spherical particles in power-law non-Newtonian media, Int. J. Miner. Process., **78**, 110-121 (2006).

ROACHE, P.J., Perspective: A method for uniform reporting of grid refinement studies, Trans. ASME, J. Fluids Engg., **116**, 405-413 (1994).

SABONI, A., ALEXANDROVA, S. AND GOURDON, C., Determination de la trainee engendree par une sphere fluide en translation, Chem. Eng. J., **98**, 175-182 (2004).

TONINI, R.D., LEMCOFF, N.O., Mass and heat transfer entry length for power-law fluids in cylindrical geometry, Letters in Heat Mass Transfr., **8**, 425-436 (1981).

TRIPATHI, A. AND CHHABRA, R.P., Drag on spheroidal particles in Dilatant fluids, AIChE J., **41**, 728-731 (1995).

TRIPATHI, A., CHHABRA, R. P. AND SUNDERARAJAN, T., Power law fluid flow over spheroidal particles, Ind. Eng. Chem. Res., **33**, 403-410 (1994).

VENU MADHAV, G. AND CHHABRA, R.P., Drag on non-spherical particles in viscous fluids, Int. J. Miner. Process., **43**, 15-29 (1995).

WEN, Y. AND JOG, M.A., Variable property, steady, axi-symmetric, laminar, continuum plasma flow over spheroidal particles, Int. J. Heat Fluid Flow, **26**, 780-791 (2005).

WU, R.M. AND LEE, D.J., Hydrodynamic Drag on Non-Spherical Floc and Free-Settling Test, Water Res., **35**, 3226-3234 (2001).

